J Mater Sci (2011) 46:6751–6757
DOI 10.1007/s10853-011-5631-4

Thermal properties and crystallization of $PbO–MoO_3–P_2O_5$ glasses

Ivana Rösslerová · Ladislav Koudelka · Zdeněk Černošek · Petr Mošner · Ludvík Beneš

Received: 7 March 2011 / Accepted: 11 May 2011

Abstract Thermal properties and crystallization of glasses from $PbO–MoO_3–P_2O_5$ ternary system were studied in three compositional series $(100 - x)[0.5PbO–0.5P_2O_5]–xMoO_3$ (A), $50PbO–yMoO_3–(50 - y)P_2O_5$ (B), and $(50 - z)PbO–zMoO_3–50P_2O_5$ (C). Glass transition temperature, crystallization temperature, coefficient of thermal expansion, and dilatation softening temperature of the studied glasses were determined by differential thermal analysis and dilatometry. Crystallization products of annealed glass samples were investigated by X-ray diffraction and Raman spectroscopy. X-ray diffraction analysis of crystallized glasses revealed the formation of PbP_2O_6, $Pb_3P_4O_{13}$, and $PbMoO_4$ in the samples of the B series. In the series A and C in the samples with a high MoO_3 content, crystalline compounds of $Pb(MoO_2)_2(PO_4)_2$ and $(MoO_2)(PO_3)_2$, respectively, were identified. Raman spectra of crystalline samples confirmed the results of X-ray diffraction measurements and provided also information on thermal stability of glasses and formation of glass-crystalline phases in the studied glass series.

Introduction

Phosphate glasses with additions of tungsten oxide or molybdenum oxide offer prospective applications for their electrochromic properties and high ionic conductivity [1, 2]. Silver- and lithium-containing molybdato-phosphate glasses were investigated for their prospective applications as ionic conductors [3]. Phosphate glasses belong also among possible candidate materials for the vitrification of nuclear wastes with molybdenum because they possess high waste loading capacities [4, 5]. Therefore, study of their thermal behavior and the process of their crystallization are interesting for potential application of these glasses.

Chowdari et al. [3, 6, 7] reported thermal and conductivity studies of $Ag_2O–MoO_3–P_2O_5$ and $Li_2O–MoO_3–P_2O_5$ system glasses. Bih et al. [8] prepared $(1 - x)NaPO_3–xMoO_3$ glasses with $x = 0–0.5$ and studied their thermal properties, EPR and their structure from IR spectra. They found non-regular variation of the glass transition temperature, T_g, with increasing MoO_3 content with a maximum close to $x = 0.2$. Santagnelli et al. [9] studied also $(1 - x)NaPO_3–xMoO_3$ glass series, but they prepared glasses within the broader compositional region of $0 \leq x \leq 0.7$. They found also a maximum on the compositional dependence of T_g values, but much higher at $x = 0.45$. Thermal properties of $Li_2O–MoO_3–P_2O_5$ and $Na_2O–MoO_3–P_2O_5$ glasses studied Bih et al. [10] in three compositional series within the glass forming region and gave the data on glass transition temperatures and crystallization temperatures.

Lead phosphomolybdate glasses were studied by Selvaraj and Rao [11] in two compositional series $(80 - x)PbO–20P_2O_5–xMoO_3$ and $(60 - x)PbO–40P_2O_5–xMoO_3$ with 20 and 40 mol% P_2O_5. They applied DSC technique for the determination of glass transition temperature and

I. Rösslerová · L. Koudelka (✉) · Z. Černošek · P. Mošner
Department of General and Inorganic Chemistry, Faculty
of Chemical Technology, University of Pardubice,
532 10 Pardubice, Czech Republic
e-mail: ladislav.koudelka@upce.cz

L. Beneš
Joint Laboratory of Solid State Chemistry of Institute
of Macromolecular Chemistry, Academy of Sciences
of the Czech Republic and the University of Pardubice,
532 10 Pardubice, Czech Republic

heat capacity of glasses in these two compositional series of the PbO–MoO_3–P_2O_5 system. Our recent studies [12] devoted to the study of structure of glasses in the PbO–MoO_3–P_2O_5-ternary system by Raman and ^{31}P NMR spectroscopy showed on the formation of MoO_6 octahedral units in most glasses of the system, but also on the existence of tetrahedral MoO_4 units in glasses with a high MoO_3 content and a low P_2O_5 content.

In this work, thermal behavior and crystallization of glasses in the PbO-MoO_3-P_2O_5 ternary system were investigated in three compositional series starting from $Pb(PO_3)_2$ and containing $\leq$50 mol% P_2O_5.

Experimental

Glasses of the PbO–MoO_3–P_2O_5 system were prepared from reagent grade PbO, H_3PO_4 and MoO_3 in batches of 25 g. In the first stage, the reaction mixture was heated slowly in a platinum crucible up to 600 °C with the final calcination at the maximum temperature for 2 h to remove water. After the calcination the reaction mixture was heated up to the 800–1000 °C, according to the composition. After 20 min heating at the maximum temperature, the melt was cooled by pouring into a graphite mold. The obtained glasses were separately annealed for 15 min at a temperature close to their T_g and then slowly cooled to room temperature. Glass composition was checked by weighing and also by chemical analysis. The changes in the MoO_3 content were lower than 0.5 mol%. The amorphous character of the obtained glasses was checked by X-ray diffraction analysis.

Thermal behavior of glasses was studied with the DTA 404 PC (Netzsch) operating in the DSC mode at the heating rate of 10 °C min^{-1}. From the obtained, DTA curves glass transition transformation temperature, T_g^a, was determined as the onset of the change in the heat capacity, C_p, in the glass transformation region and crystallization temperature, T_c, of the glasses was determined as the onset of the exothermic crystallization peak. The measurements were carried out on powder samples with a mean diameter 8–10 μm placed in silica crucibles under an atmosphere of N_2. The thermal expansion coefficient, α, the glass transition temperature, T_g, and dilatation softening temperature, T_d, were measured on bulk samples with dimensions of 25 × 5×5 mm using dilatometer DIL 402 PC (Netzsch). From the obtained dilatation curves, the coefficient of thermal expansion, α, was determined as a mean value in the temperature range of 100–200 °C, the glass transition temperature, T_g^b, was determined from the change in the slope of the elongation versus temperature plot and the dilatation softening temperature, T_d, was determined as the maximum of the expansion trace corresponding to the onset of viscous deformation. The dilatometric measurements were carried out in air at the heating rate of 5 °C min^{-1}.

Glass crystallization was studied by annealing the powdered glass samples at temperatures slightly above their crystallization peak for 2 h. Crystalline products were identified by X-ray diffraction analyses of annealed samples on Bruker D8 Advance X-ray diffractometer with the application of PDF 4 database for the determination of crystalline products.

Annealed samples were also analyzed by Raman spectroscopy for the identification of glass-crystalline phases. The Raman spectra were measured at room temperature using Horiba Jobin-Yvon LabRam HR spectrometer. The spectra were recorded in back-scattering geometry under excitation with He–Ne laser radiation (632.8 nm) at a power of 12 mW. The spectral slit width was 1 mm, exposure time was 3 s and accumulation number was 10.

Results and discussion

We have prepared 14 glass samples of the PbO–MoO_3–P_2O_5 ternary system by slow cooling of the corresponding melt in air to room temperature. Their amorphous character was confirmed by X-ray diffraction. We have studied changes in their thermal properties in three compositional series $(100 - x)[0.5PbO–0.5P_2O_5]–xMoO_3$ (series A), 50 PbO–$yMoO_3$-$(50 - y)P_2O_5$ (series B) and $(50 - z)PbO–zMoO_3–50P_2O_5$ (series C). Their composition is shown in Table 1. Glass samples containing MoO_3 were of blue color showing on the presence of Mo^{5+} species in the glasses which was confirmed by EPR spectroscopy. The EPR studies also showed that the ratio of Mo^{5+}/Mo^{total} in most samples is lower than 0.9%.

DSC curves obtained for the glass series (A) are shown in Fig. 1. The values of glass transition temperature, T_g^a and crystallization temperature T_c, determined from DSC curves are given in Table 1. We have determined glass transition temperature by two methods. From DSC curves, T_g^a values were determined as the intersection between the extrapolated line of the glass heat flow before T_g and the extrapolated line of the changing heat flow in the glass transition region, according to the procedure proposed by Yue [13]. The values of T_g^a determined by this procedure from the onset of the change in heat flow on DSC curves in the glass transformation region are very close to T_g^b values obtained from the change in the slope of the elongation versus temperature plot of the dilatometric measurements in agreement with [13]. In Table 1, the values of both T_g are given. On some DSC curves also endothermic peaks of

Table 1 Compositions of studied glasses and their glass transition temperature, T_g^a (onset on the DSC curve), T_c^a (onset of crystallization peak), criterion of thermal stability of glasses, $T_c^a - T_g^a$, glass transition temperature, T_g^b (measured by dilatometry), dilatation softening temperature, T_d^b, and thermal expansion coefficient, α, of PbO–MoO_3–P_2O_5 glasses

Samples	PbO (mol%)	MoO_3 (mol%	P_2O_5	$T_g^a \pm 2$ (°C)	$T_c^a \pm 2$ (°C)	$T_c^a - T_g^a$ (°C)	$T_g^b \pm 2$ (°C)	$T_d^b \pm 2$ (°C)	α ± 0.5 (ppm/°C) (100–200 °C)
Series A	50	0	50	309	401	92	310	330	17.9
	45	10	45	340	545	205	338	352	16.5
	40	20	40	364	–	–	362	378	15.6
	35	30	35	401	–	–	399	407	15.2
	30	40	30	418	608	190	416	430	14.1
	25	50	25	420	592	172	417	435	13.7
	20	60	20	392	528	136	394	411	14.0
	15	70	15	367	464	97	365	379	14.4
Series B	50	0	50	309	401	92	310	330	17.9
	50	10	40	350	520	170	351	373	17.1
	50	20	30	409	550	141	408	427	16.1
	50	30	20	420	490	70	418	435	15.9
Series C	50	0	50	309	401	92	310	330	17.9
	40	10	50	338	550	212	338	352	13.4
	30	20	50	395	627	232	396	422	13.0
	20	30	50	310	528	218	310	336	11.9

melting of the crystallized glasses can be seen with their characteristic temperature T_m, usually determined as the onset of the endothermic peaks.

In the (A) series $(100 - x)[0.5PbO–0.5P_2O_5]–xMoO_3$ $(0 < x<70)$ under slow cooling in air, we prepared glasses in the compositional range of 0–70 mol% MoO_3. Their glass transition temperature, according to DTA measurements, increases with increasing MoO_3 content from 309 °C with increasing MoO_3 content and reaches a maximum of 420 °C at the glass with 50 mol% MoO_3 and then decreases. The T_g values obtained from dilatometric curves (Table 1) are close to those determined from DSC curves as the onset of the change in heat flow in the glass transition region (Fig. 1). As the changes in ΔC_p within the glass transition region on the DSC curves of glasses with $x = 40–70$ mol% MoO_3 in Fig. 1 are too small, the magnified part of the DSC curves is shown in Fig. 2 together with an example of the determination of T_g. Most glasses

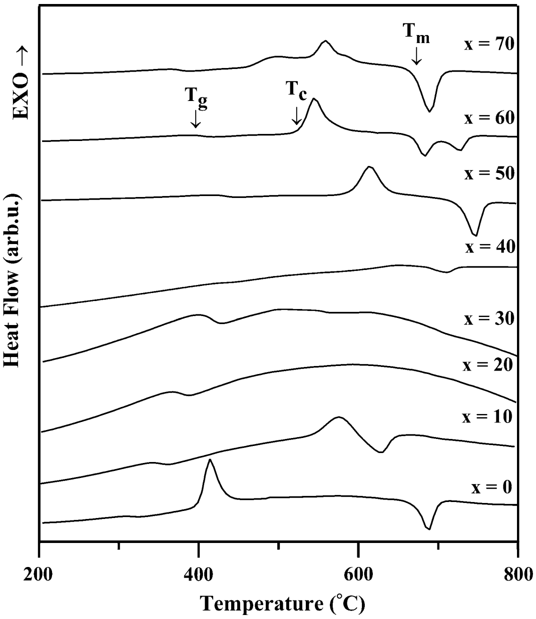

Fig. 1 DSC curves of the glass series $(100 - x)[0.5PbO–0.5P_2O_5]–xMoO_3$ (A series). The values of T_g and T_c are given in Table 1

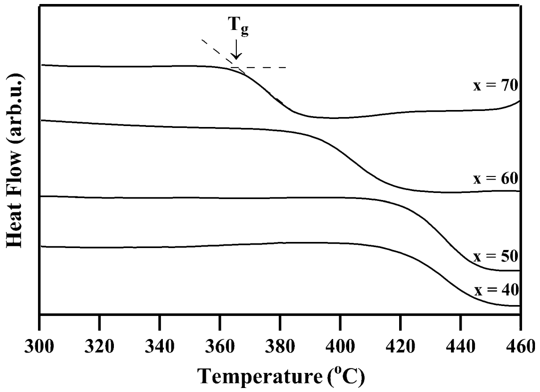

Fig. 2 Part of DSC curves of the glass series $(100 - x)[0.5PbO–0.5P_2O_5]–xMoO_3$ (A series) magnified for the demonstration of the determination of T_g^a values for the samples with $x = 40–70$ mol% MoO_3

crystallize on heating as manifested on DSC curves in Fig. 1 by the presence of an exothermic crystallization peak. Crystallization temperatures determined as the onset of the crystallization peak are also given in Table 1. Most thermally stable glasses in this series are those containing 20–30 mol% MoO_3 which do not crystallize on heating. Coefficient of thermal expansion decreases with increasing MoO_3 content from 17.9 ppm/°C down to 13.7 ppm/°C at the glass with 50 mol% MoO_3 and then slowly increases. Glass transition temperature in the series (B) 50PbO–yMoO_3-(50 − y)P_2O_5 also increases with increasing MoO_3 content and reaches a maximum of 420 °C at the glass with 30 mol% MoO_3, whereas thermal expansion coefficient decreases but goes down only to 15.9 ppm/°C (see Table 1). In the glass series (C) (50 − z)PbO–$z$$MoO_3$–50$P_2O_5$, the T_g and T_c values increase within the range of 0-–20 mol% MoO_3 and then decrease, whereas thermal expansion coefficient goes rapidly down.

In order to indentify products of crystallization of the studied glasses, we have milled the glass samples and heat treated the obtained powder for 2 h at temperatures slightly above their corresponding crystallization peaks. The annealing temperatures are given in Table 2 together with the composition of crystalline phases identified by X-ray diffraction analysis in all three glass series. For the identification of the results of crystallization, we have applied also the Raman spectroscopy and the obtained Raman spectra are shown in Figs. 3, 6, and 7.

In the glass series (A) (100 − x)[0.5PbO–0.5P_2O_5]–$x$$MoO_3$ in samples with 0–10 mol% MoO_3 the only crystalline phase identified in crystallization products by X-ray diffraction was lead metaphosphate PbP_2O_6. Raman spectra also revealed the presence of crystalline lead metaphosphate with characteristic strong vibrational bands of 1150 and 670 cm^{-1} [14]. Raman spectrum of the glass with $x =$ 10 mol% MoO_3 (Fig. 3) shows within the region of 820–980 cm^{-1} also the presence of two broad Raman bands characteristic of the presence of molybdate structural units in the glassy phase [15, 16]. It means that the annealed sample contains one crystalline phase (PbP_2O_6) and one glassy phase containing MoO_3. Glasses with x = 20–30 mol% MoO_3 are thermally stable and do not reveal any crystallization peak on DSC curves on heating with the heating rate of 10 °C/min. Also their annealing at three different temperatures did not result in their crystallization as revealed by X-ray diffraction and their Raman spectra (Fig. 3) reveal only the presence of glassy phase with two dominant broad bands within the region of 850–970 cm^{-1} ascribed to vibrations of molybdate units [15, 16]. DSC curve on heating the sample with x = 40 mol% MoO_3 does not show any visible crystallization peak, but shows a weak endothermic melting peak at 696 °C which reveals a partial crystallization of the glassy sample. X-ray diffraction analysis of annealed samples with x = 40 and 50 mol% MoO_3 identified the presence of one crystalline phase of the composition of $Pb(MoO_2)_2(PO_4)_2$. Its composition corresponds exactly to

Table 2 Annealing temperatures and crystallization products of glasses of the system PbO–MoO_3–P_2O_5

Samples	PbO (mol%)	MoO_3 (mol%)	P_2O_5 (mol%)	T_c (°C)	Products of crystallization (PDF No. [24])
Series A	50	0	50	480	PbP_2O_6 (04-010-2426)
	45	10	45	580	PbP_2O_6 (04-010-2426)
	40	20	40	490, 550, 600	–
	35	30	35	490, 550, 600	–
	30	40	30	600	$Pb(MoO_2)_2(PO_4)_2$ (04-012-8283)
	25	50	25	600	$Pb(MoO_2)_2(PO_4)_2$ (04-012-8283)
	20	60	20	560	$Pb(MoO_2)_2(PO_4)_2$ (04-012-8283) MoO_3 (00-005-0508)
	15	70	15	560	$Pb(MoO_2)_2(PO_4)_2$ (04-012-8283) MoO_3 (00-005-0508)
Series B	50	0	50	480	PbP_2O_6 (04-010-2426)
	50	10	40	540	$Pb_3P_4O_{13}$ (04-010-1540)
	50	20	30	560	$Pb(MoO_2)_2(PO_4)_2$ (04-012-8283) $Pb_2P_2O_7$ (00-043-0469)
	50	30	20	505	$PbMoO_4$ (01-074-1075)
Series C	50	0	50	480	PbP_2O_6 (04-010-2426)
	40	10	50	570	PbP_2O_6 (04-010-2426)
	30	20	50	490	PbP_2O_6 (04-010-2426)
	20	30	50	570	$(MoO_2)(PO_3)_2$ (01-074-1389)

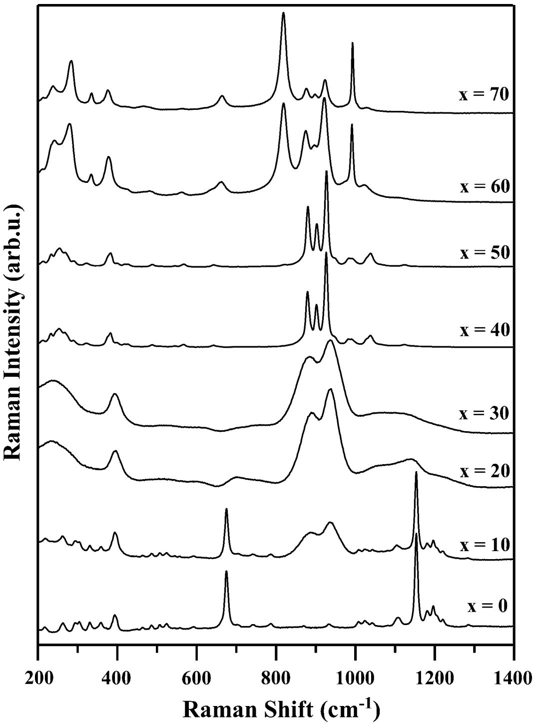

Fig. 3 Raman spectra of the annealed $(100 - x)[0.5PbO–0.5P_2O_5]–xMoO_3$ samples (A series). Crystalline phases identified by XRD in the annealed samples are given in Table 2

the glass with $x = 50$ mol% MoO_3 and on its DSC curve, there is one exothermic peak of crystallization and one endothermic melting peak. In the annealed samples of glasses with $x = 60$ and 70 mol% MoO_3 X-ray diffraction found the presence of the compound $Pb(MoO_2)_2(PO_4)_2$ and crystalline MoO_3. The DSC curve of the sample with $x = 60$ mol% MoO_3 (Fig. 1) shows two melting peaks which corresponds to the presence of two crystalline phases. Raman spectra of these samples (Fig. 3) are in good agreement with the results of XRD.

We have devoted our attention also to the compound of $Pb(MoO_2)_2(PO_4)_2$. Its structure was determined by Masse et al. [17]. This compound is interesting for the study due to its ability to form glassy state. As the chemical composition of the melt and the corresponding crystalline phase are the same, it is possible to evaluate the processes of crystallization and melting. On the bases of several DTA measurements with the heating rate within the range of 5–20 °C/min in the first step the activation energy of crystallization was determined as $E_c^* = 308 \pm 3$ kJ/mol (3.19 ± 0.03 eV) with the application of Kissinger method [18]. In the second step, we have applied obtained data also for the evaluation of an appropriate kinetic model of the crystallization process. We have found that the crystallization kinetics can be described by the Šesták-Berggren model SB(m, n) [19] with parameters of $m = 0.88 \pm 0.18$ $n = 1.52 \pm 0.31$.

We have determined also melting temperature of the $Pb(MoO_2)_2(PO_4)_2$ compound as $T_m = 706 \pm 3$ °C, peak temperature of the melting process was $T_{p,m} = 747 \pm 7$ °C. Melting enthalpy was determined as $\Delta H_m = 39.7 \pm 1.4$ J/g. We have also evaluated glass transformation process in the glass of this composition. Glass transition temperature increases with increasing heating rate from 417 °C (5 °C/min) to 424 °C (20 °C/min). Activation energy of glass transition process was evaluated also with the application of Kissinger method [18] as $E_{T_g}^* = 496 \pm 39$ kJ/mol (5.14 ± 0.51 eV). The change in the isobaric heat capacity at the glass transition is $\Delta C_p = 0.138$ J/(g K).

In Fig. 4, there is a comparison of Raman spectra of polycrystalline compound $Pb(MoO_2)_2(PO_4)_2$ and the corresponding glass. Raman spectra of the polycrystalline compound are in a good agreement with the tabular data of Raman spectra given by Isaac et al. [20]. From Fig. 4, it is evident that the main features of the Raman spectrum of the glass can be obtained by broadening the bands of the Raman spectrum of the crystals corresponding to fluctuations of bonding angles and bond lengths in the disordered glassy network. From the similarity of basic spectral features of both spectra, we can assume that the short-range order in the glass is similar to that in the crystal $Pb(MoO_2)_2(PO_4)_2$ and that basic structural units in both phases are probably the same.

In the (B) series of glasses $50PbO–yMoO_3–(50 - y)P_2O_5$ under slow cooling in air, we prepared glasses in the compositional range of 0–30 mol% MoO_3. Their glass transition temperature increases also with increasing MoO_3 content by 111 °C as shown on DSC curves in Fig. 5. All glasses crystallize on heating and the difference $T_c - T_g$ is the highest at the glass with $y = 10$ mol% MoO_3. Crystallization temperatures determined as the onset of

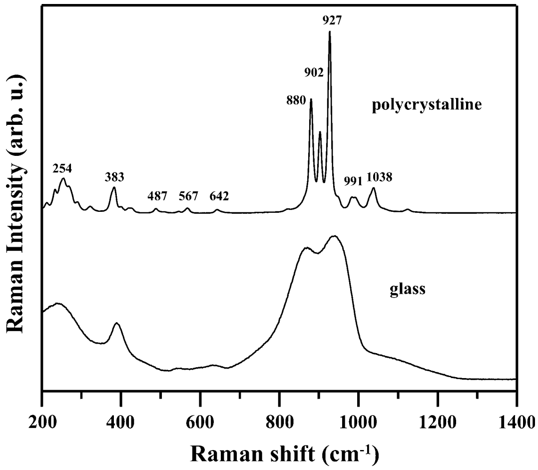

Fig. 4 Raman spectra of the polycrystalline $Pb(MoO_2)_2(PO_4)_2$ compound and the $50[0.5PbO–0.5P_2O_5]–50MoO_3$ glass

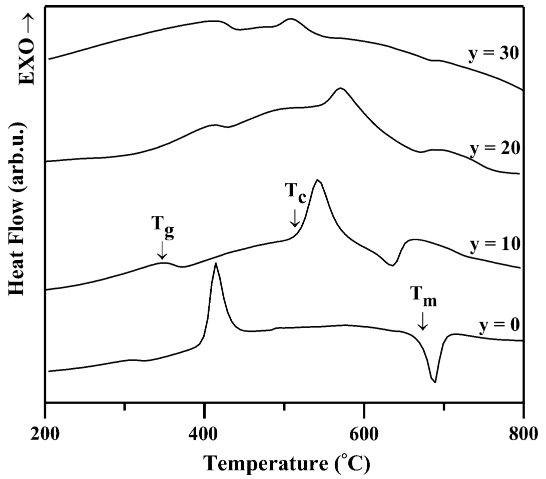

Fig. 5 DSC curves of the glass series $50PbO–(50 - y)P_2O_5–yMoO_3$ (B series). The values of T_g and T_c are given in Table 1

crystallization peak are given in Table 1. X-ray diffraction revealed various products formed in the annealed samples (Table 2). Crystalline PbP_2O_6 is formed only in the crystallized pure lead metaphosphate glass, whereas in the sample with $y = 10$ mol% MoO_3 the presence of lead tetraphosphate $Pb_3P_4O_{13}$ was identified. Lead diphosphate $Pb_2P_2O_7$ is formed in the annealed sample with $y = 20$ mol% MoO_3 together with the compound $Pb(MoO_2)_2(PO_4)_2$ identified also in the series A. The XRD analysis of the crystallized sample with $y = 30$ mol% MoO_3 identified lead molybdate $PbMoO_4$ as the only crystalline phase. It means that some lead phosphate remained in the glassy state here. Raman spectra of the annealed samples (Fig. 6) are in good agreement with the results of XRD analysis. In the sample with $x = 10$ mol% MoO_3 molybdate phase remains amorphous as evidenced by a broad Raman band within the region of 850–970 cm^{-1}. The presence of crystalline phase $Pb(MoO_2)_2(PO_4)_2$ is evident in the annealed simple with $y = 20$ mol% MoO_3, where characteristic Raman bands are similar to those shown in Fig. 5.

In the (C) series of glasses $(50 - z)PbO–zMoO_3–50P_2O_5$, we prepared glasses with $z = 0–30$ mol% MoO_3. Thermal analysis showed here also an increase in the glass transition temperature with increasing MoO_3 content, but both T_g and T_c values at the glass with $z = 30$ mol% MoO_3 are lower. Previous study [11] revealed in this glass a high content of Mo^{5+} ions, the presence of which according to Flower et al. [21] weakens the glass network, as Mo^{5+} ions occupy network-modifying positions in the glass structure and decrease the rigidity of the glass network. This conclusion could explain decreased values of T_g in the glass $20PbO–50P_2O_5–30MoO_3$. Coefficient of thermal expansion decreases here with increasing MoO_3 content as shown in Table 1.

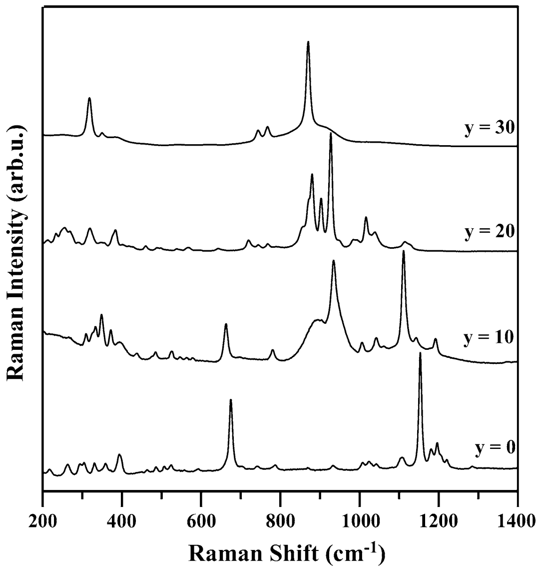

Fig. 6 Raman spectra of the annealed $50PbO–(50 - y)P_2O_5–yMoO_3$ samples (B series). Crystalline phases identified by XRD in the annealed samples are given in Table 2

XRD analysis identified in the annealed samples with $z = 0–20$ mol% MoO_3 only PbP_2O_6 as the crystalline phase, whereas molybdate phase remained amorphous as evidenced from the Raman spectra (Fig. 7) of these samples by the presence of two broad bands within the range of 850–970 cm^{-1}. In the sample with $z = 30$ mol%, MoO_3 crystalline phase of the composition $(MoO_2)(PO_3)_2$ was identified by XRD analysis. This result is in agreement with the Raman spectra of annealed samples (Fig. 7), where the characteristic band of the compound $(MoO_2)(PO_3)_2$ at 984 cm^{-1} was observed. This dominant Raman band

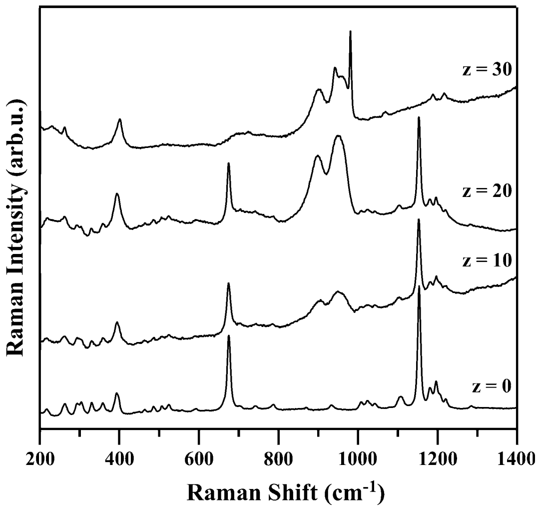

Fig. 7 Raman spectra of the annealed $(50 - z)PbO–50P_2O_5–zMoO_3$ samples (C series). Crystalline phases identified by XRD in the annealed samples are given in Table 2

corresponds to the dominant band in the Raman spectrum of the $(MoO_2)(PO_3)_2$ compound published by Morgan and Magruder [22]. The structure of crystalline $(MoO_2)(PO_3)_2$ contains MoO_6 octahedra and chains of PO_4 units [23]. Annealed sample with $z = 30$ mol% MoO_3 contains a part of the sample in the glassy state as evidenced in its Raman spectrum by the presence of a broad Raman bands within the range of 850–1000 cm^{-1}.

Conclusion

Study of thermal behavior and crystallization of PbO–MoO_3–P_2O_5 ternary system glasses by combined techniques of thermal analysis, X-ray diffraction, and Raman spectroscopy showed to be very effective from the point of characterization of annealed samples. DSC studies showed on a good thermal stability of glasses of the A series with 20–30 mol% MoO_3, which do not crystallize on heating or annealing. Basic characterization of crystalline products by XRD is naturally most important. Nevertheless, Raman spectroscopy is able not only to verify obtained crystalline products, but also to detect the existence of glassy phases in the samples which do not crystallize completely. Crystallization of some glassy samples showed on the formation of crystalline lead molybdato-phosphate compound $Pb(MoO_2)_2(PO_4)_2$ in some glasses with a high MoO_3 content. We assume that some structural motifs of this compound are present in the corresponding glasses. In the P_2O_5-rich crystallized samples, another compound $(MoO_2)(PO_3)_2$ was identified, the structure of which contains MoO_6 octahedra and PO_4 tetrahedra, and we are convinced that short-range order in crystalline and glassy phases is the same.

Acknowledgements The authors are grateful for the financial support from the research project No. P106/10/0283 of the Grant Agency of Czech Republic and from the research project No. 0021627501 of the Ministry of Education of Czech Republic.

References

1. Zakis YR, Lusis AR, Lagzdons YL (1982) J Non-Cryst Solids 47:267
2. Studer F, Lebail A, Raveau B (1986) J Solid State Chem 63:414
3. Chowdari BVR, Gopalakrishnan R, Tang SH, Kuok SH (1988) Solid State Ion 28–30:704
4. Pinet O, Dussossoz JL, David C, Fillet C (2008) J Nucl Mater 377:307
5. Chourasia R, Shrivastava OP, Wattal PK (2009) J Alloys Comp 473:579
6. Chowdari BVR, Tan KL, Chia WT, Gopalakrishnan R (1990) Solid State Ion 40–41:684
7. Chowdari BVR, Tan KL, Chia WT, Gopalakrishnan R (1991) J Non-Cryst Solids 128:18
8. Bih L, Nadiri A, El Amraoui Y (2005) J Phys IV Fr 123:165
9. Santagneli SH, de Araujo CC, Strojek W, Eckert H, Poirier G, Ribeiro SJL, Messadeq Y (2007) J Phys Chem B 111:10109
10. Bih L, Nadiri A, Aride J (2002) J Therm Anal Calorim 68:965
11. Selvaraj U, Rao KJ (1988) J Non-Cryst Solids 104:300
12. Koudelka L, Rösslerová I, Holubová J, Mošner P, Montagne L, Delevoye L (2011) J Non-Cryst Solids. doi:10.1016/j.jnoncrysol.2011.03.006
13. Yue Y-Z (2008) J Non-Cryst Solids 354:1112
14. Bobovich YaS (1962) Opt Spektrosk 13:459
15. Chowdari BVR, Tan KL, Chia WT (1993) Mater Res Soc Symp Proc 293:325
16. Šubčík J, Koudelka L, Mošner P, Montagne L, Trickot G, Delevoye L, Gregora I (2010) J Non-Cryst Solids 356:2509
17. Masse R, Averbuch-Pouchot MT, Durif A (1985) J Solid State Chem 58:157
18. Kissinger HE (1957) Anal Chem 29:1702
19. Šesták J, Berggren G (1971) Thermochim Acta 3:1
20. Isaac M, Jayasree V, Suresh G, Nayar VU (1992) Ind J Phys B 66:65
21. Flower GL, Baskaran GS, Reddy MS, Veeraiah N (2007) Phys B 2393:61
22. Morgan SH, Magruder RH (1990) J Am Ceram Soc 73:753
23. Kierkegaard P (1961) Ark Kemi 18:521
24. Joint Committee on Powder Diffraction Standards, International Centre of Diffraction Data, Swarthmore, PA, USA